Angewandte Zuschriften

Colloidal Crystals

Deutsche Ausgabe: DOI: 10.1002/ange.201500273
Internationale Ausgabe: DOI: 10.1002/anie.201500273

Non-Brownian Particle-Based Materials with Microscale and Nanoscale Hierarchy**

Melissa H. Lash, Jahnelle C. Jordan, Laura C. Blevins, Morgan V. Fedorchak, Steven R. Little, and Joseph J. McCarthy**

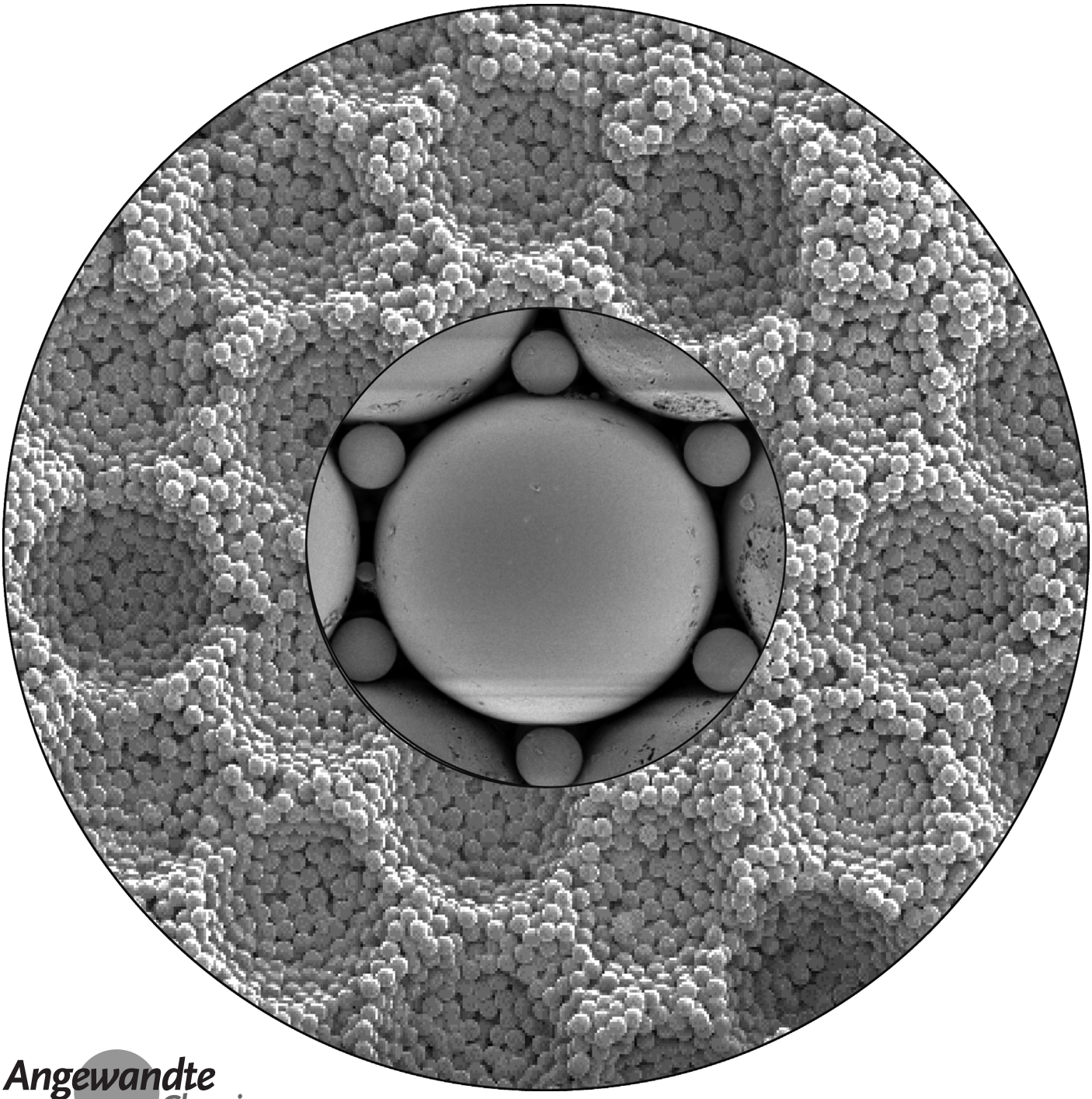

Angewandte Chemie

© 2015 Wiley-VCH Verlag GmbH & Co. KGaA, Weinheim

Abstract: *Colloidal crystals are interesting materials owing to their customizable photonic properties, high surface area, and analogy to chemical structures. The flexibility of these materials has been greatly enhanced through mixing particles with varying sizes, compositions, and surface charges. In this way, distinctive patterns or analogies to chemical stoichiometries are produced; however, to date, this body of research is limited to particles with nanoscale dimensions. A simple method is now presented for bottom-up assembly of non-Brownian particle mixtures to create a new class of hierarchically-ordered materials that mimic those found in nature (both in pore distribution as well as stoichiometry). Additionally, these crystals serve as a template to create particle-based inverted crystalline structures with customizable properties.*

Binary and higher-order multicomponent colloidal crystals (bCC and mCC, respectively) are organized arrays of particles with highly customizable architectures (feature sizes and shapes) as well as hierarchy.[1,2] They can be produced from combinations of uniform (monodispersed) particle populations of either the same or differing materials. These arrays have historically been produced by entropy-driven self-assembly of sub-micrometer or nanoscale particles for use in applications such as photonics (bandgap materials), chemical or biological sensing, and microelectronics, where their nanoscale features enhance their functionality.[3] The breadth of applications where hierarchically porous structures are useful can reach far beyond those dependent solely on nanoscale features.[4–7] However, as the diameter of the particle increases, self-assembly occurs over a much slower time scale and becomes irrelevant as a naturally-driven crystallization method. Thus systematic fabrication of materials that span beyond the sub-micrometer scale has been elusive.[5,8,9] At the other end of the spectrum, for millimeter-scale (and larger) particles (granular), a driving force, such as vibration, is essential to overcome the natural barriers to particle motion and arrangement.[10] Recently, we showed that one can bridge this gap in materials fabrication by using ultrasonic agitation to mimic Brownian motion (or granular vibration), and induce spontaneous assembly of microspheres with dimensions ranging from the nano- to the milliscales into hexagonal close-packed (HCP) two- and three-dimensional crystals.[11] Herein, we extend this bottom-up assembly approach to mixed systems of particles that include a span in length scale that is larger than any explored to date to attain complex hierarchical crystalline formations from binary and multicomponent particle mixtures. By doing so, we have created stoichiometric configurations of large, non-Brownian particles that resemble those formed naturally by atoms and molecules and heretofore have been reported only for nanoparticles.[12–14] Specifically, we examine a range of radii ratios ($\gamma_{S/L}$) and number ratios ($N_{S/L}$) of small (S) and large (L) microparticles within a mixture to explore a wide range of resulting microstructures. Additionally, through post-processing of these microstructures, we have demonstrated that it is possible to evolve these ordered arrays into binary, inverted crystalline structures with customizable hierarchically ordered features and pore configurations that mimic those in naturally occurring porous materials (such as zeolites).

In the context of particle self-assembly, the understanding of interparticle interactions is crucial to interpreting particle phenomena.[11,15,16] Many parameters, including the particle material composition/density, size, and charge, are key contributors to such behavior, especially in particle mixtures[13] where size mismatch has also been shown to strongly influence the resultant particle structures.[16] In fact, in hard sphere (screen-charged) mixtures of nanoscale particles, it has been observed that $\gamma_{S/L}$ and $N_{S/L}$ determine whether the system attains a stoichiometric or amorphous configuration.[1,13,16–19] Many experimental studies show that bCCs can only be produced when $0.154 < \gamma_{S/L} < 0.225$; however, simulation results suggest that $0.3 < \gamma_{S/L} < 0.41$ should be possible.[3] Recently, Cai et al. have experimentally expanded the working size ratio to $\gamma_{S/L} = 0.376$ through convective assembly to produce non-close packed binary crystals.[3,20] For mixtures with particle size ratios ranging from the large particle being three to five times larger than the small particles, entropic ordering has been widely cited as a strong driving force among sub-micrometer sized particles.[21,22]

Conversely, in granular mixtures, particle behavior is dependent on an external force (usually a vibration) to induce particle movement.[10] Typically the thermal energy in the system ($k_B T$) is orders of magnitude smaller than the energy required to move that particle an appreciable distance. However, oftentimes when binary particle mixtures are vibrated, a separation phenomenon known as the "Brazil nut effect" (large particles rise to the top and small particles sink to the bottom), is often observed.[23–25] Between each vibration, various metastable configurations may exist in the particle bed and these states last until the next vibration occurs.[10,11,25,26] Several factors affect the mixing/segregation behavior of large granular particles, including the frequency and amplitude of the vibration as well as the mass, density, diameter ratio of binary mixture, and the inter-particle and particle-wall coefficients of friction.[26]

Less is known about the assembly behavior of large, non-Brownian microparticles than nano- and granular (centi/milli-) scale particle behavior. Self-assembly of nanoscale components is usually limited to bottom-up methods while larger components are assembled by top-down methods.[27] Microscale particles lie in the middle, however, with a great deal of untapped potential as building blocks to be manipulated in the creation of macroscale functional materials. By employing self-assembly to organize non-Brownian particles,

[*] M. H. Lash, J. C. Jordan, L. C. Blevins, Dr. M. V. Fedorchak, Dr. S. R. Little, Dr. J. J. McCarthy
Chemical and Petroleum Engineering, University of Pittsburgh
3700 O'Hara St, Pittsburgh PA 15261 (USA)
E-mail: srlittle@pitt.edu
jjmcc@pitt.edu

[**] M.H.L. was supported by the U.S. Dept. of Ed. GAANN PR/Award No: P200A100087. The National Science Foundation's REU funding supported J.C.J. (EEC-1359308) and L.C.B. (EEC-1005048). We thank the Center for Biological Imaging at the U. of Pittsburgh for use of their SEM, and S. Mahoney and Prof. G. Veser for help with and use of their high-temperature oven.

Supporting information for this article is available on the WWW under http://dx.doi.org/10.1002/anie.201500273.

 © 2015 Wiley-VCH Verlag GmbH & Co. KGaA, Weinheim

microparticle-based structures can be created with new opportunities for varying macroscopic hierarchy, surface functionalization, and the diffusive properties. Engineering these aforementioned properties allows the design of novel materials for applications for which nanoscale features are not suitable. Herein we explore a new method of creating autonomously assembled, microparticle-based crystals from particles with varying dimensions and compositions. Specifically, we employ sonication as a means of artificially thermally treating a system of large, non-Brownian microparticles such that we induce organization among particles up to 0.1 mm in size.[11] Furthermore, we observe that it is possible to produce a variety of predictable stoichiometric patterns (corresponding to $N_{S/L}$) from particles that are two to three orders of magnitude larger than those previously studied. We have achieved particle organization for mixtures containing particles as small as $d_S = 0.6$ μm and as large as $d_S = 21$ μm combined with $d_L = 100$ μm, where d is particle diameter, and S and L represent the small and large particle populations, respectively. By further increasing the $\gamma_{S/L}$ above 0.21, we have formed crystals among particles where $d_S =$ 21 μm and $d_L = 75$ μm, yielding a ratio of $\gamma_{S/L} = 0.28$. However, as $\gamma_{S/L}$ increases, the likelihood for organization and achieving stoichiometric patterns decreases, as suggested in previous studies of submicrometer-sized particles in the literature.[28] As such, we did not experimentally observe any pattern formation or long-range organization when exploring particle combinations where $\gamma_{S/L} > 0.28$ or from particle populations with a dispersity, or particle size distribution above 5%. The process for producing these crystals is described in the Supporting Information, Figure S1. While we refer to these crystals as bCCs and mCCs to follow with the nanoparticle naming convention, we acknowledge that the particles used are non-colloidal (due to size).

In the crystallization process, a particle mixture in deionized water (DIW) is deposited at room temperature on a flat substrate and agitated by ultrasonic waves from a sonication bath. The sonication effects can be altered by changing the bath medium, the substrate, and the sonication solvent.[11] In this work we tested a variety of substrates including flat glass coverslips (both hydrophobic and hydrophilic), a cubic plastic mold, and a cylindrical glass vial; however, the bCC and mCC results shown throughout this work are produced on a flat hydrophilic glass substrate for ease of imaging (although qualitatively similar crystallization occurred with all substrates). When preparing samples for sonication, the volume of each particle solution (either polystyrene (PS) or soda lime glass (SL)) can be altered prior to mixing. We do not observe measurable differences when varying the volume (V) ratio across a reasonably wide range of values (a factor of five, as determined by measuring the center-to-center distances among the large particles in the resultant structures); however, larger changes in the volume ratio (more than five times) result in drastically different structures, depending on the number of large particles available and the area over which they were dispersed (data not shown).

Within each crystalline domain, we note a lack of overall homogeneity, as highlighted in Figure 1 A. We hypothesize

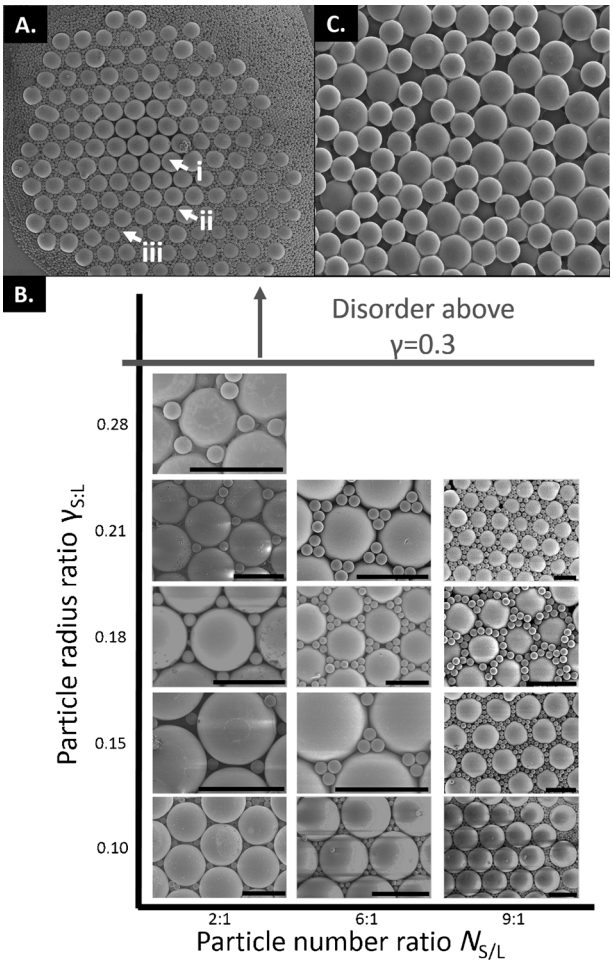

Figure 1. A) Representative overview image of a crystalline domain of 100 μm SL and 21 μm PS particles. The arrows i, ii, and iii indicate different phases within the local regions on the sample. B) Structural configurations formed at various radius ratios, ranging from $0.1 < \gamma_{S/L} < 0.28$. C) Disordered packing observed between particles outside of a feasible number (stoichiometric) range that would be expected to produce order (21 μm and 15 μm in size, with $\gamma_{S/L} = 0.71$). All scale bars are 100 μm.

that this heterogeneity is due to variations in local particle concentration resulting from improper mixing of the component particles (similar to observations in Dai et al.).[29] Specifically, we observe a tendency for the small particles to form a layer on the substrate below the binary crystal (verified on inverted light microscope). At the same time, within the binary crystal, the concentration of small particles is often greater around the edges of the crystalline domain (Figure 1 A). Despite inhomogeneity in particle mixing, the local variations in $N_{S/L}$ result in the expected configurations for these ratios, as highlighted by arrows in Figure 1 A and with images in Figure 1 B (where they are further correlated with variations in $\gamma_{S/L}$).

These areas of short-range order occur for $0.10 < \gamma_{S/L} <$ 0.28. When the radius ratio is below 0.1 we observe closely packed structures of the larger particles, with space-filling from the smaller particles, but ultimately no discernable stoichiometric pattern formation (Supporting Information, Figure S2). Stoichiometric pattern formation was not

 © 2015 Wiley-VCH Verlag GmbH & Co. KGaA, Weinheim

observed at this lower bound owing to a geometric limitation, where the smaller particles are too small to remain in the larger particle interstitial spaces. On the other end of the stoichiometric spectrum, Figure 1C depicts the amorphous particle arrangement that is typical for size ratios close to unity (here, $\gamma_{S/L} = 0.71$), where instead of acting like independent particle populations, the two particle sizes behave more like a single non-uniform population, thereby leading to disorder. Other incidents of disorder arise from the formation of defects and cracks in the crystalline structure. We suspect that the formation of defects for these non-Brownian bCCs occurs in a similar way to defect formation among nanoparticle mixtures and monodispersed particle-based crystals. The formation of defects and cracks may develop due to the competition between the dense crystal structure formation versus the hydrodynamic pressure in the fluid evaporation process, non-uniformity in particle size, or changes in the orientational configuration (for example, a switch between HCP and FCC).[18,30]

The methods described herein can be extended for the creation of multicomponent crystals of varying $\gamma_{S/M/L}$ (Figure 2). Many combinations of triphasic crystals should be feasible provided that a given phase and its nearest co-mixture population are within the observed size ratio ranges that allow crystallization (for example, $\gamma_{S/M,\ \gamma_{M/L}} \leq 0.3$, but > 0.1). The mCC structures shown here are created by sonication on a flat substrate with all particle solutions in equal volume ratios.

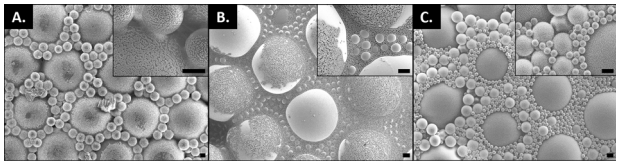

Figure 2. mCC structures created by sonication on a flat glass substrate. Triphasic mixtures were made from A) 0.6, 18, and 100 μm particles, B) 1, 10, and 100 μm particles, and C) 6, 18, and 100 μm particles. All scale bars are 10 μm.

We have also been able to form inverse hierarchical crystals similar to those formed on the nanoscale.[14,31–33] Inverted colloidal crystals (ICC) are widely studied and fabricated with nanoparticles as well as with larger particles.[14,34–37] However, in all previously reported studies, the ICC backbone is comprised of a continuous solid material (usually a polymer).[20,32,38,39] Here, we demonstrate the novel use of fused, smaller particles serving as the backbone material to the ICC, creating an open and interconnected network known as a particle-based ICC. Figure 3 depicts these structures formed from fused 1, 10, or 21 μm polystyrene particles that remain after etching away the 100 μm soda lime particles. The original binary crystal was co-assembled as described previously, however an excess of the smaller particles was used to achieve a higher degree of sample homogeneity (bCC and particle-based ICC seen in the Supporting Information, Figure S3). These structures are observed to have long-range order over a large area, as

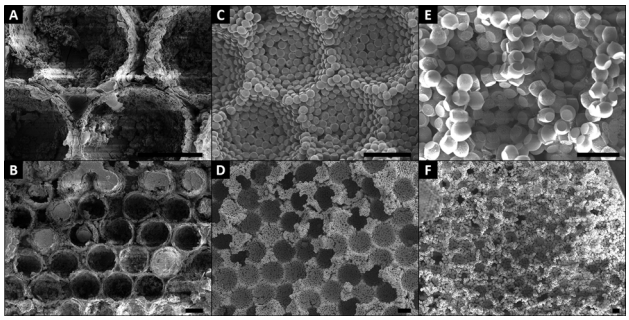

Figure 3. Inverted crystal composed of polystyrene particles after removal of 100 μm SL particles by a 5% HF/DIW washing sequence. The ICCs are made of A), B) 1 μm particles, C), D) 10 μm particles, and E), F) 21 μm particles. All scale bars are 50 μm.

shown in Figure 3B,D,F. Within these particle-based ICCs, 1) niche microenvironments form in the large spherical cavities; 2) an innate interconnectivity emerges from the porous nature of the crystalline walls composing the scaffold; and 3) an increased internal surface area can be achieved by optimizing particle and fusion point size.

By agitating particles in a way that can overcome gravitational and kinetic limitations, we have shown that conventional applications of self-assembly typically employed at the atomic and nanoscale can be translated to the microscale where the impact of Brownian forces are negligible. Furthermore, this mimicry of natural thermal processes can be used in the creation of larger-scale multicomponent crystals and the formation of their inverse structures. These structures can be produced from particles of varying sizes and materials, allowing rapid, bottom-up creation of hierarchical (and porous) materials that would traditionally be produced through a (potentially lengthy and costly) top-down approach. Additionally, their macroscopic shape can be easily engineered by varying the substrate shape in the fabrication process. These materials offer new opportunities for creating customizable and self-assembled niche microenvironments for drug delivery and tissue engineering, as well as new acoustic dampening, battery, and filtration materials, among others. Additionally, they resemble naturally derived materials such as zeolites and biological tissue (for example, bone, cartilage, and lung), owing to their high surface area, bidispersed pore distribution, and multilevel hierarchy.[39–41] Translation of such materials will require scaling up the crystallization process. Further investigation into the mechanism behind microparticle mixture organization may allow for the creation of large crystalline domains with long-range order within bCC, mCC, and particle-based ICC structures.

Keywords: colloidal crystals · microparticles · multicomponent crystals · nanostructures · self-assembly

How to cite: *Angew. Chem. Int. Ed.* **2015**, *54*, 5854–5858
Angew. Chem. **2015**, *127*, 5952–5956

[1] G. Singh, S. Pillai, A. Arpanaei, P. Kingshott, *Adv. Funct. Mater.* **2011**, *21*, 2556–2563.
[2] X. Ye, L. Qi, *Sci. China Chem.* **2014**, *57*, 58–69.

 © 2015 Wiley-VCH Verlag GmbH & Co. KGaA, Weinheim

[3] Z. Cai, Y. J. Liu, X. Lu, J. Teng, *ACS Appl. Mater. Interfaces* **2014**, *6*, 10265 – 10273.
[4] H. Yang, X. Dou, Y. Fang, P. Jiang, *J. Colloid Interface Sci.* **2013**, *405*, 51 – 57.
[5] G. M. Whitesides, B. A. Grzybowski, *Science* **2002**, *295*, 2418 – 2421.
[6] G. M. Whitesides, M. Boncheva, *Proc. Natl. Acad. Sci. USA* **2002**, *99*, 4769 – 4774.
[7] M. Boncheva, D. Bruzewicz, G. M. Whitesides, *Pure Appl. Chem.* **2003**, *75*, 621 – 630.
[8] N. B. Crane, O. Onen, J. Carballo, Q. Ni, R. O. Guldiken, *Microfluid. Nanofluidics* **2013**, *14*, 383 – 419.
[9] C. X. Li, X. Z. An, R. Y. Yang, R. P. Zou, A. B. Yu, *Powder Technol.* **2011**, *208*, 617 – 622.
[10] E. Nowak, J. Knight, E. Ben-Naim, H. Jaeger, S. Nagel, *Phys. Rev. E* **1998**, *57*, 1971 – 1982.
[11] M. H. Lash, M. V. Fedorchak, S. R. Little, J. J. McCarthy, *Langmuir* **2015**, *31*, 898 – 905.
[12] E. C. M. Vermolen, A. Kuijk, L. C. Filion, M. Hermes, J. H. J. Thijssen, M. Dijkstra, A. van Blaaderen, *Proc. Natl. Acad. Sci. USA* **2009**, *106*, 16063 – 16067.
[13] N. J. Lorenz, H. J. Schöpe, H. Reiber, T. Palberg, P. Wette, I. Klassen, D. Holland-Moritz, D. Herlach, T. Okubo, *J. Phys. Condens. Matter* **2009**, *21*, 464116.
[14] J. Wang, Q. Li, W. Knoll, U. Jonas, *J. Am. Chem. Soc.* **2006**, *128*, 15606 – 15607.
[15] K. J. M. Bishop, C. E. Wilmer, S. Soh, B. A. Grzybowski, *Small* **2009**, *5*, 1600 – 1630.
[16] F. Li, D. P. Josephson, A. Stein, *Angew. Chem. Int. Ed.* **2011**, *50*, 360 – 388; *Angew. Chem.* **2011**, *123*, 378 – 409.
[17] J. Zheng, Z. Dai, F. Mei, X. Xiao, L. Liao, W. Wu, X. Zhao, J. Ying, F. Ren, C. Jiang, *J. Phys. Chem. C* **2014**, *118*, 20521 – 20528.
[18] L. Wang, Y. Wan, Y. Li, Z. Cai, H. Li, X. Zhao, Q. Li, *Langmuir* **2009**, *25*, 6753 – 6759.
[19] T. Muangnapoh, A. L. Weldon, J. F. Gilchrist, *Appl. Phys. Lett.* **2013**, *103*, 181603.
[20] Z. Cai, J. Teng, Y. Wan, X. S. Zhao, *J. Colloid Interface Sci.* **2012**, *380*, 42 – 50.
[21] J. S. Vesaratchanon, A. Nikolov, D. Wasan, D. Henderson, *Ind. Eng. Chem. Res.* **2009**, *48*, 6641 – 6651.
[22] R. Dickman, P. Attard, V. Simonian, *J. Chem. Phys.* **1997**, *107*, 205 – 213.
[23] A. Jain, M. J. Metzger, B. J. Glasser, *Powder Technol.* **2013**, *237*, 543 – 553.
[24] M. J. Metzger, B. Remy, B. J. Glasser, *Powder Technol.* **2011**, *205*, 42 – 51.
[25] R. Brito, R. Soto, *Eur. Phys. J.* **2009**, *179*, 207 – 219.
[26] Z. Xie, P. Wu, S. Wang, Y. Huang, S. Zhang, S. Chen, C. Jia, C. Liu, L. Wang, *Soft Matter* **2013**, *9*, 5074 – 5086.
[27] R. Thiruvengadathan, V. Korampally, A. Ghosh, N. Chanda, K. Gangopadhyay, S. Gangopadhyay, *Rep. Prog. Phys.* **2013**, *76*, 066501.
[28] N. Vogel, L. de Viguerie, U. Jonas, C. K. Weiss, K. Landfester, *Adv. Funct. Mater.* **2011**, *21*, 3064 – 3073.
[29] Z. Dai, Y. Li, G. Duan, L. Jia, W. Cai, *ACS Nano* **2012**, *6*, 6706 – 6716.
[30] S. V. Karpov, I. L. Isaev, a. P. Gavrilyuk, V. S. Gerasimov, a. S. Grachev, *Colloid J.* **2009**, *71*, 329 – 339.
[31] J. Wang, S. Ahl, Q. Li, M. Kreiter, T. Neumann, K. Burkert, W. Knoll, U. Jonas, *J. Mater. Chem.* **2008**, *18*, 981 – 988.
[32] M. Retsch, U. Jonas, *Adv. Funct. Mater.* **2013**, *23*, 5381 – 5389.
[33] Y. Wan, Z. Cai, L. Xia, L. Wang, Y. Li, Q. Li, X. S. Zhao, *Mater. Lett.* **2009**, *63*, 2078 – 2081.
[34] J. E. Nichols, J. Cortiella, J. Lee, J. A. Niles, M. J. Cuddihy, S. Wang, J. Bielitzki, A. Cantu, R. Mlcak, E. Valdivia, et al., *Biomaterials* **2009**, *30*, 1071 – 1079.
[35] N. A. Kotov, Y. Liu, S. Wang, C. Cumming, *Langmuir* **2004**, *20*, 7887 – 7892.
[36] C. M. Andres, M. L. Fox, N. A. Kotov, *Chem. Mater.* **2012**, *24*, 9 – 11.
[37] S.-W. Choi, Y. Zhang, M. R. Macewan, Y. Xia, *Adv. Healthcare Mater.* **2013**, *2*, 145 – 154.
[38] Y. Zhang, K. Regan, Y. Xia, *Macromol. Rapid Commun.* **2013**, *34*, 485 – 491.
[39] Y. S. Zhang, S.-W. Choi, Y. Xia, *Soft Matter* **2013**, *9*, 9747 – 9754.
[40] B. Suki, R. Lutchen, *J. Appl. Physiol.* **1994**, *76*, 2749 – 2759.
[41] M. J. Cuddihy, N. A. Kotov, *Tissue Eng. Part A* **2008**, *14*, 1639 – 1649.

Received: January 12, 2015
Published online: April 20, 2015

 © 2015 Wiley-VCH Verlag GmbH & Co. KGaA, Weinheim